

## Early damage detection in planetary gear transmission in different operating conditions

Ayoub Mbarek<sup>a,b</sup>, Alfonso Fernández<sup>b</sup>, Ahmed Hammami<sup>a</sup>, Fakher Chaari<sup>a</sup>, Fernando Viadero<sup>b</sup>, Mohamed Haddar<sup>a</sup>

<sup>a</sup> Mechanics, Modelling and Production Laboratory, National School of Engineers Sfax, Tunisia  
[ayoubmbarekenit@gmail.com](mailto:ayoubmbarekenit@gmail.com)

<sup>b</sup> Department of Structural and Mechanical Engineering, Faculty of Industrial and Telecommunications Engineering, University of Cantabria, Santander, Spain

### Abstract

Planetary gear transmissions are sensitive to various running environmental factors. These external conditions keep these systems often subjected to faults and/or malfunction especially in gears components. So, it is a crucial task to spot in advance all kind of degradation that could lead to a harmful event or accident to the system. In the same context, this study aims to investigate the case of combined faults detection and analyse their impact on the vibration dynamic response in a two stages planetary gear transmission in diverse operating conditions. For this, a Lumped Mass Model (LMM), referred to a real test rig where experimental tests, is established. In this model, the Time Varying Mesh Stiffness (TVMS) were modelled in different frameworks and configurations such as the healthy, the single and the combined damage conditions. After acquiring acceleration signals from the model, time, frequency and order analysis data processing were executed to generate health related data for the planetary gear. Consequently, it is concluded that the system vibration response is sensitive to the internal excitation particularly the case of combined defects. The obtained results show the ability of the developed model to identify the frequency characteristics of defect and the transmission in each configuration. The experimental and simulated results are compared and correlated.

**Keywords:** planetary gear, faults, steady-state, vibration; non-stationary regime.

### 1-Introduction

Gearbox systems are a principal component in many mechanical engineering applications like wind turbine and automotive industry, they are characterised by their ability to transmit a high important power with a multiplication of input speed and/or load. Diagnosis based on vibration is an interesting and efficient option to identify and understand the behaviour of a mechanical system, [1].

After a long time, hard exploitation, gears are subjected to various kind of teeth damages such as crack and spalling which affect the reliability of the system. These failures impact also on the principal source of excitation in gearbox systems which is the TVMS. Generally, the failure status would be reflected by changes on these functions, [2]. Likewise, Ma et al. [3] reviewed the impact of crack and spalling failure on TVMS. The modelling of these functions caused by tooth crack, is computed using the empirical approach [4]. Chaari et al. [5] used an analytical formula to model TVMS in presence of crack damage. In Liang et al, [6] work, an analytical method to compute the meshing function in presence of pitting failure considering the severity of pitting was proposed. Moreover, Ma et al. [7], Saxena et al. [8] reported the influence of shape and its location of rectangular spalling on TVMS. All studies agreed that a tooth damage can be modelled by a drop down in the amplitude of TVMS [9, 10]. Generally, these functions will be exploited later to study the dynamic behaviour of the gearbox system.

In fact, influences of gear failure on the dynamic behaviour were generously investigated. For further insight on condition monitoring of the complex mechanical system, many kinds of research and investigations were carried out. A nonlinear mathematical dynamic model was developed by Cheng et al. [13] to investigate the behaviour in case of a cracked carrier plate.

Time and frequency domain vibration signals were developed, and fault features were extracted. Tian et al. [14] used a 6 DOF LMM in order to study the dynamic response of a one-stage gearbox in presence of crack failures. Liang and Zuo. [15] utilized an 18 DOF of lumped model to investigate vibration properties of a planetary gear with a cracked tooth in a planet gear in the time and frequency domains. Li et al. [16] developed crack detection techniques for a multistage gear set using dynamics-based simulation and experimental investigation. Moreover, Ryali and Talbot [17] developed a lumped mass model considering the elastic mesh contact in the inner excitation to study the dynamic response of planetary gear transmission.

Considering the effect of crack on the dynamic behaviour, Chen and Shao [18] established a 6 DOF of a spur gear system. The same model was also used by Mohammed et al. [19] to discuss the effect of tooth crack propagation on the dynamic response of a gear system. Besides, Wu et al. [20] used a 6 DOF model of a gear system to analyse the effects of crack on the system vibration response. Mohammed et al. [21] developed a 12 DOF gear dynamic model including the gyroscopic and friction effects. To investigate dynamic characteristics of the system when the crack in the pinion grows, Zhou et al. [22] adopted a 16 DOF mathematic model, which is developed by Howard et al. [23] for a one-stage gear system.

Moreover, gear faults diagnostic techniques are addressed in several studies [24, 27]. Some works were focusing on extracting the frequencies characteristic of the failures to localize gear failures [24-25]; while in other research the features of frequency domain were used to determine the failure gear [26-27]. Thus, many others developed wavelet transformation methods for failure detection [28-33]. Besides, Hong and Dhupia [34] proposed a novel approach for gear failure detection based on combining Kurtosis and fast dynamic time method. Fedala et al. [35] use angular measurements to diagnose different gear faults.

Research on gear faults detection in planetary gear transmission are generally addressed in the case of a single damage diagnosis by a numerical approach or experimental measurement as reported in many scientific papers like in Park et al works, [36]. In fact, the authors used a numerical approach based on transmission errors functions to study the dynamic behaviour of a planetary gear transmission and to diagnosis faults. Li et al. [37] analysed the impact of the crack geometrical form of the sun gear on the TVMS and the dynamic behaviour of a multistage planetary gear transmission using numerical and experimental approach. Later, Li et al. [38] concentrated to study the influence of chipped gear on the dynamic behaviour using a nonlinear model. Recently, Sang et al. [39] studied numerically the impact of detects components location of the vibration response of a 3K-II planetary gear system.

Early faults detection is always a challenge for research in order to avoid a bad scenario like the apparition of novel damage which can cause more degradation and a malfunction of the transmission. As mentioned previously, the majority of research are widely addressed to the aspect of only one defect detection. In the presented paper, early combined defect detection is investigated numerically and experimentally in back to back planetary gear system. The developed model shows a good capability to describe and to reflect the reality. It allows the analysis of the dynamic behaviour in different operating conditions such as healthy, one defect and combined defects in stationary and non-stationary regimes. Practically, the gear faults characteristics are complicated especially in the case of a complex planetary gear set where the frequency components are close to each other's. Indeed, gear faults identification is established in the case of a non-stationary external excitation. The obtained results show that the order tracking technique can be used for fault identification and localization of the planetary gear transmission.

Generally, under normal regimes, the signals coming from the transducer would be preceded and information could then extract. However, the non-stationary regimes and failure events complicate deeply the monitoring of these systems. However, the researches addressed to combined defects and spalling defects detection in non-stationary regimes of epicyclic gear are limited, whether its modelling of TVMS, its impact on response vibration and the efficient techniques for detection. This paper focuses on this gap. It aims to study and analyse the dynamic behaviour of two stages gear sets is in presence of planet spalling and crack faults in a steady state where the external load and input speed are constant over time and in start-up regime. The paper is organised as follow:

In section 1, the used experimental test rig and the developed model are presented, and their associated parameters are detailed. Also, this section is dedicated to the modelling of failures. In section 2, the impact of faults on the vibratory response are highlighted, the measured and simulated vibration response are analysed in time and frequency domain in healthy condition and in presence of defects. Section 3 is focused on spalling defect detection in start-up regime.

**2- Experimental set up:**

In this work, an experimental test rig is used during measurement process, (Figure 1). It has a special configuration widely used in wind turbine gearbox systems or aircraft transmission. This design allows the conservation of power and facilitates the recirculation of energy in the gear components,(Carrier(c),Ring (r),Sun (s), Planets (1,2,3)).

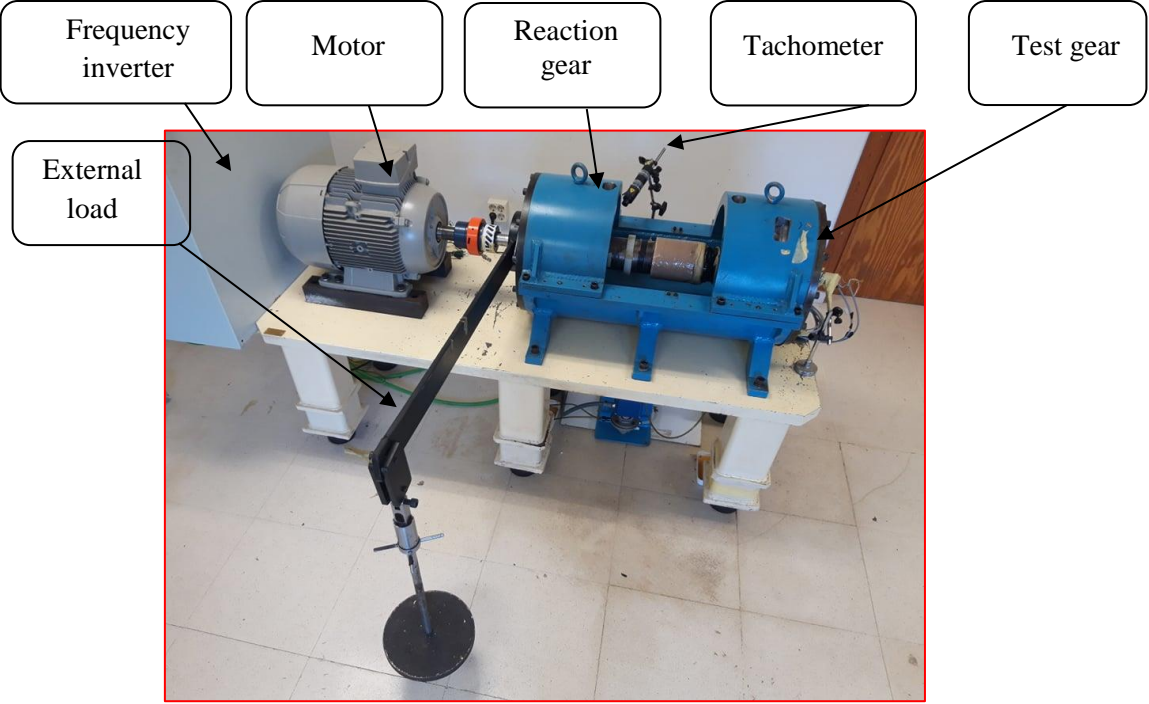
The test rig is basically composed by two stages planetary gears supported by a rigid housing and connected by two rigid hubs, a synchronous motor to drive the gear, and a frequency inverter in order to monitor the speed. The torque is applied by adding plate on a rigid arm attached to the reaction gear, Figure 1.

During measurement test, several instrumental accessories are mounted of the bench like tachometer, sensors and slip ring as shown in Figure 2.

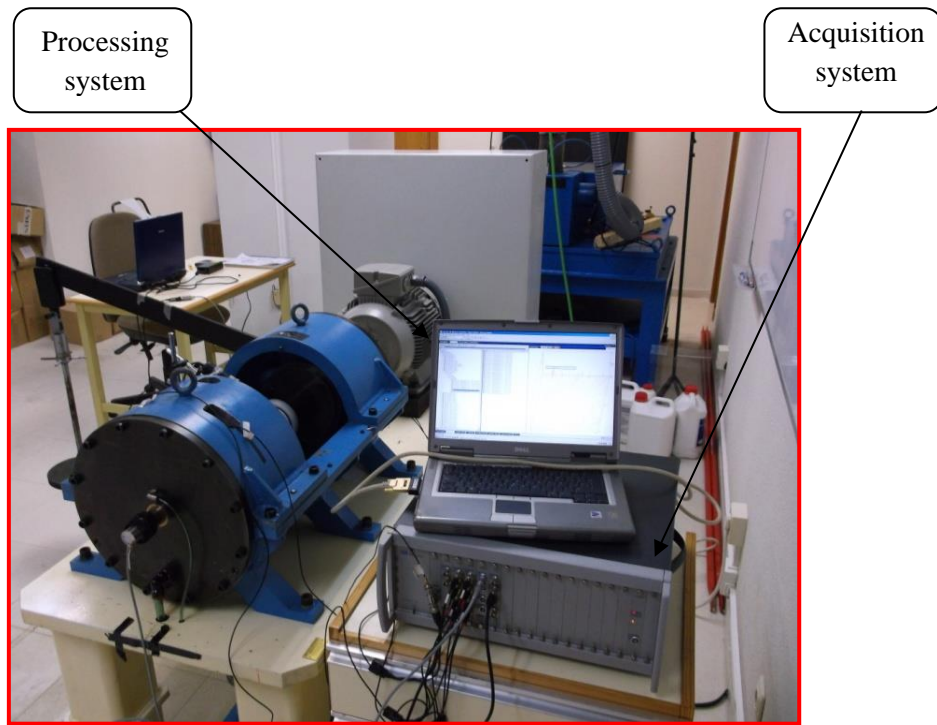
To do that, four tri-axial accelerometers (ENDEVCO /65M-100/10023) with high sensitivity as shown in table 1 were used and fixed on the reaction gear set and the test ring.

The sensors are mounted on the tangential direction of test ring in order to measure the accelerations responses which are proceeded using LMS test lab acquisition system.

More details concerning the test bench are well detailed in [40-42].



(a)



(b)  
**Fig.1.** (a) Test rig (b) Acquisition and Processing system

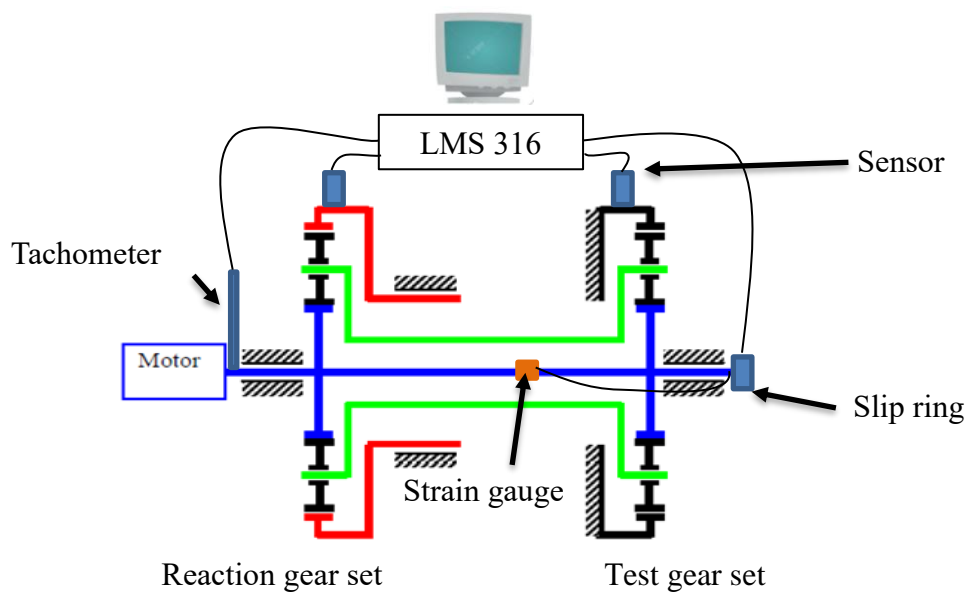


**Fig.2.** Scheme of the test rig

The test rig dynamic behaviour is established in different operating conditions such as without or in presence of defects, in steady or non-stationary conditions. In fact, two kinds of failures which are the spalling and the crack, are examined separately and combined.

The spalling failure is situated on one of the planets, it has a rectangular parallelepiped form, whereas the crack is implemented at the sun tooth. The geometrical details of gear components are listed in the table 2.

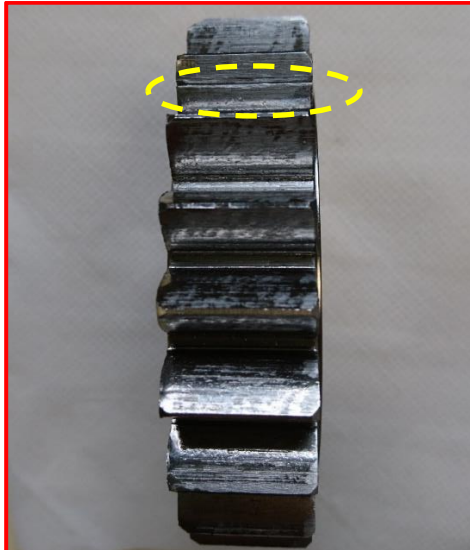


**Fig. 3.** Spalling on the planet gear



**Fig. 4.** Crack on the test sun gear

**Table 1:** Accelerometers characterization

	1	2	3	4
Serial number	10020	10021	10022	10023
X-Sensitivity (mV/g )	102.6	103.5	101.6	101.6
Y-Sensitivity (mV/g )	101.3	98.68	99.67	103.0
Z-Sensitivity (mV/g )	101.1	104.3	102.6	101.9



Where  $i=c,r,s,p1,p2,p3$ .

The global mass matrix  $M$  is diagonal matrix considering the mass and inertia terms of gear elements.

$$M = \text{diag} \left[ \frac{I_{cr}}{r_{cr}} + N \cdot m_{pr}, \frac{I_{rr}}{r_{rr}}, \frac{I_{sr}}{r_{sr}}, \frac{I_{pr}}{r_{pr}}, \frac{I_{pr}}{r_{pr}}, \frac{I_{pr}}{r_{pr}}, \frac{I_{ct}}{r_{ct}} + N \cdot m_{pt}, \frac{I_{rt}}{r_{rt}}, \frac{I_{st}}{r_{st}}, \frac{I_{pt}}{r_{pt}}, \frac{I_{pt}}{r_{pt}}, \frac{I_{pt}}{r_{pt}} \right] \quad (5)$$

Viscous Damping is assumed in the model using Rayleigh's model, the coefficients ( $\alpha$ ,  $\beta$ ) are taken such that conservative [43].

In Eq 1,  $K$  is the effective stiffness of the system, which combine the TVMS  $K_e(t)$  and the bearing stiffness.

$$K(t) = \begin{bmatrix} K_r(t) & 0 \\ 0 & K_t(t) \end{bmatrix} \quad (6)$$

$$K_t(t) = \begin{bmatrix} \sum_{i=1}^3 (K_{sti}(t) + K_{rti}(t)) & -\sum_{i=1}^3 K_{rti}(t) & -\sum_{i=1}^3 K_{rti}(t) & K_{rt1}(t) - K_{st1}(t) & K_{rt2}(t) - K_{st2}(t) & K_{rt3}(t) - K_{st3}(t) \\ -\sum_{i=1}^3 K_{rti}(t) & \sum_{i=1}^3 K_{rti}(t) & 0 & -K_{rt1}(t) & -K_{rt2}(t) & -K_{rt3}(t) \\ -\sum_{i=1}^3 K_{sti}(t) & 0 & \sum_{i=1}^3 K_{sti}(t) & K_{st1}(t) & K_{st2}(t) & K_{st3}(t) \\ K_{rt1}(t) - K_{st1}(t) & -K_{rt1}(t) & K_{st1}(t) & K_{st1}(t) + K_{rt1}(t) & 0 & 0 \\ K_{rt2}(t) - K_{st2}(t) & -K_{rt2}(t) & K_{st2}(t) & 0 & K_{st2}(t) + K_{rt2}(t) & 0 \\ K_{rt3}(t) - K_{st3}(t) & -K_{rt3}(t) & K_{st3}(t) & 0 & 0 & K_{st3}(t) + K_{rt3}(t) \end{bmatrix} \quad (7)$$

$$K_r(t) = \begin{bmatrix} \sum_{i=1}^3 (K_{sri}(t) + K_{rri}(t)) & -\sum_{i=1}^3 K_{rri}(t) & -\sum_{i=1}^3 K_{rri}(t) & K_{rr1}(t) - K_{sr1}(t) & K_{rr2}(t) - K_{sr2}(t) & K_{rr3}(t) - K_{sr3}(t) \\ -\sum_{i=1}^3 K_{rri}(t) & \sum_{i=1}^3 K_{rri}(t) & 0 & -K_{rr1}(t) & -K_{rr2}(t) & -K_{rr3}(t) \\ -\sum_{i=1}^3 K_{sri}(t) & 0 & \sum_{i=1}^3 K_{sri}(t) & K_{sr1}(t) & K_{sr2}(t) & K_{sr3}(t) \\ K_{rr1}(t) - K_{sr1}(t) & -K_{rr1}(t) & K_{sr1}(t) & K_{sr1}(t) + K_{rr1}(t) & 0 & 0 \\ K_{rr2}(t) - K_{sr2}(t) & -K_{rr2}(t) & K_{sr2}(t) & 0 & K_{sr2}(t) + K_{rr2}(t) & 0 \\ K_{rr3}(t) - K_{sr3}(t) & -K_{rr3}(t) & K_{sr3}(t) & 0 & 0 & K_{sr3}(t) + K_{rr3}(t) \end{bmatrix} \quad (8)$$

Following the kinematic configuration of the system, either the sun is the input, and the carrier is the output, the external force  $F(t)$  is expressed as follow:

$$F_i(t) = [F_c, 0, F_s, 0, 0, 0]^T \text{ with } i=r,t \quad (9)$$

Effectively, the developed model simulates the vibratory behaviour of the test bench as multiple DOF of mass damper spring system. The internal excitations due to the teeth contact between S-P and R-P generate vibration along with the meshing process. However, in presence of failure, these vibrations increase which makes the characterization of defects features difficult especially in non-stationary running cases. In fact, modelling of TVMS under these conditions is required allowing the analysis of the dynamic response of the system.

#### 4-Influence of faults on TVMS:

##### a-Spalling defect:

In this section, it is desired to study the impact of faults on TVMS in the steady state regime and start up regimes.

In literature and as mentioned in the introduction, the TVMS can be modelled using several methods such as the finite element method, the energy method and the square waveform method.

Because we are interested in the impact of the defect on the vibration response of gear system, the square waveform is adopted considering the meshing process i.e. the TVMS are stationary functions respecting the alternative contact between the single tooth and double teeth. Unfortunately, these functions cannot be measured experimentally when the system is in service.

Under damage condition, a drop down in TVMS is presented. This phenomenon is explained to the decreasing contact area between a healthy tooth and the damaged tooth. In the studied case, the fault is located only on one planet of the test gear. So, only the trend of (*S-PI*) and (*S-PI*) will be modified respecting the period of the faults  $T_{dp}$ .

The planet fault was modelled as indicated by [23], by reducing the width of the tooth and as outcome an increasing of the deflection due to the bending as displayed in Fig.6.

Based on the shape of the input speed and respecting the period of the defect, TVMS were computed and created as displayed in the following figures.

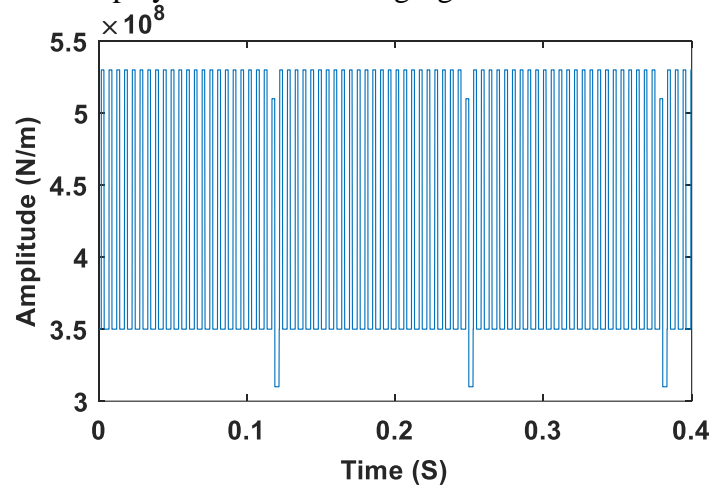


**Fig.6.** R-P1 trend in spalling defects case

**b-Cas of combined defects:**

The TVMS are also modelled in case of combined teeth defects, spalling defects as explained previously and then a crack defect mounted on the sun of the test gear.

The fact that the spalling failure is on the planet 1, and a crack failure is situated on the sun, (*R-P1*) function will be affected by two kinds of drop down of amplitude following the period of each defect and the severity of damage as illustrated in Fig 7. In addition, a reduction on the (*S-P1*) function is occur.

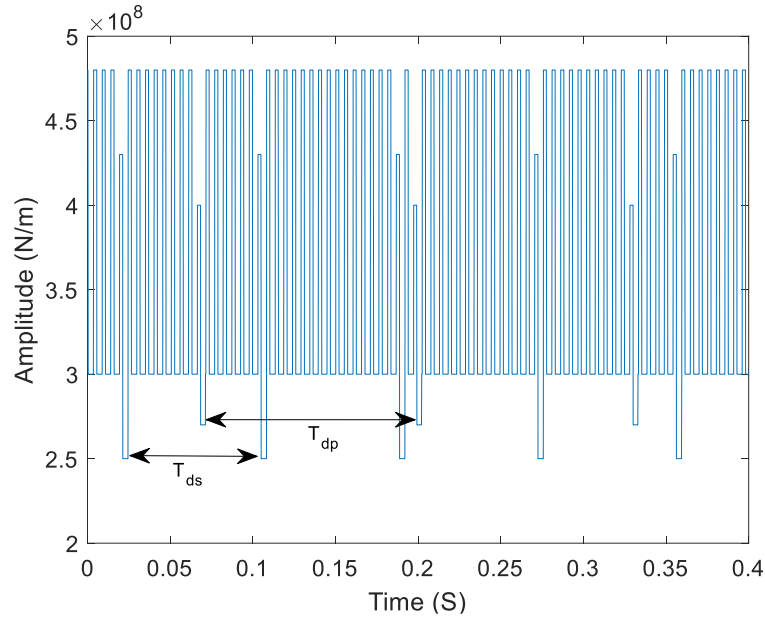


**Fig.7.** R-P1 trend in combined defects case

## 5-2- Fault effect on the dynamic response:

### 5-2-1-Stationary condition:

During this regime, the bench is driven with a fixed speed of 890 rpm and fixed load 600 N-m. Also, the sampling frequency is fixed to 1000 Hz and 10s for the sample time. All the measured and the simulated accelerations signals are recorded on the angular direction of the test ring. The gearbox system is exposed to different and independent sources of excitation coming from several paths and independent like the GMF and the movement of the faulty planet. All the features frequencies of these excitations are listed in table 3.

**Table 3.** Frequencies characteristic of planetary gear components.

Type	Test		
Natural frequency $N_f$ (Hz)	352 / 364/ 386 / 406/ 413		
Components	P	C	S
Associated frequency (Hz)	6,9	3	35,3
Mesh frequency (Hz)	191		

### a-Healthy condition:

In Fig.8, the time response of accelerations trend is represented, a modulation amplitude is observed for both simulated and experimental responses. This fact is explained to two principal factors which are the mesh phase relation between the planet components, which was considered in the numerical model and also to the force due to the rotation of the carrier as reported in [38]. This force can be simulated as sinusoidal function which consider the mesh relation, the force is maximal when the planets are close to the sensors and minimal when they are far. Also, the vibration amplitude is constant over time because several hypotheses are considered such as that the planets components are identical, all gear components are modelled as a rigid body.

To get more insight on the frequency characterisation, the spectrum of the vibration response is illustrated in figure 9.

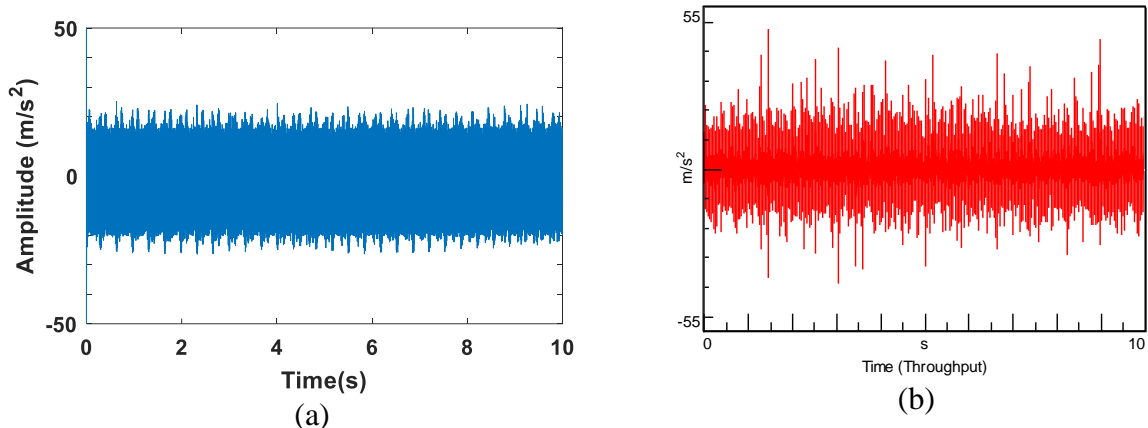


**Fig.8.** Time response (a) Simulated (b) Measured

The modulation amplitude in figure 8 is translated by a modulation of frequency in figure 9, it can be observed that the GMF which is the main source of excitation of gear system and its harmonic is modulated by several sidebands. These one is principally due to rotation of carrier components are presented with a very low amplitude. To get more insight to be able to interrupt the obtained results, a zoom around the second GMF is selected to study the sidebands features.

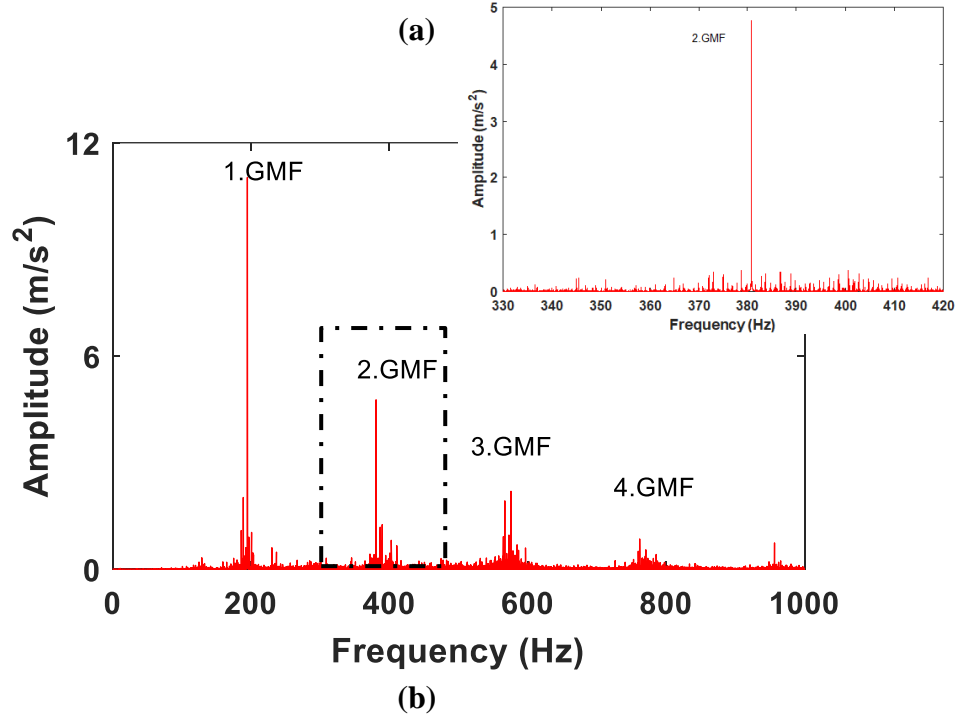
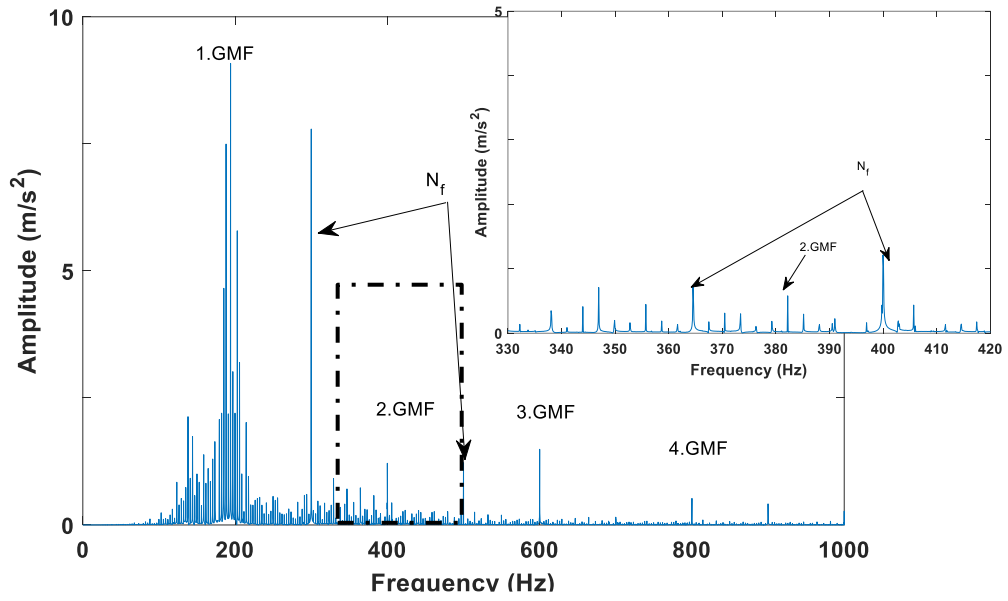


**Fig.9.** Spectrum (a) Simulated (b) Measured

The results illustrated in figure 9 show that the 1st GMF is dominating, this behaviour is explained by several factors such as the used input load during experiments and simulation. The load influences the domination of the GMF as reported in Hammami et al. [44]. In their work, authors studied the influence of load on the dynamic behaviour of a planetary gear system. The obtained results show that with the variation of load the dominating GMF can be change. However, in the studied case, the introduced load is low which cause a domination of the 1<sup>st</sup> GMF on the spectrum as illustrated in figure 9.

In addition, this behaviour is related to the modulation phenomena due to the passage of the planet gear around the sensors fixed on the ring.

**b-Planet Spalling defect state :**

Some information's could be distinguished from Fig 10 is that the amplitudes of accelerations are increased comparing to the healthy case. Also, it can be seen that when the damaged tooth enters in contact with another tooth, periodic "impulses" appear in the vibratory response. The period  $T_{dp}$  related to the damaged tooth is difficult to identify on both simulated and measured time response. Additionally, Fig.10 (b) presents a clear larger number of peaks compared to Fig.10 (a). This is principally explained by several influenced factors like the white noise presented during experimental tests.

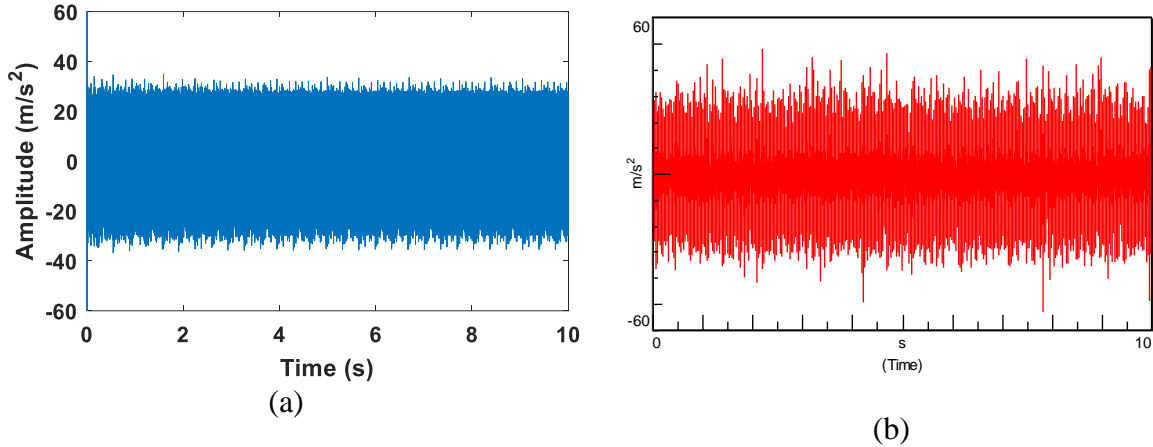
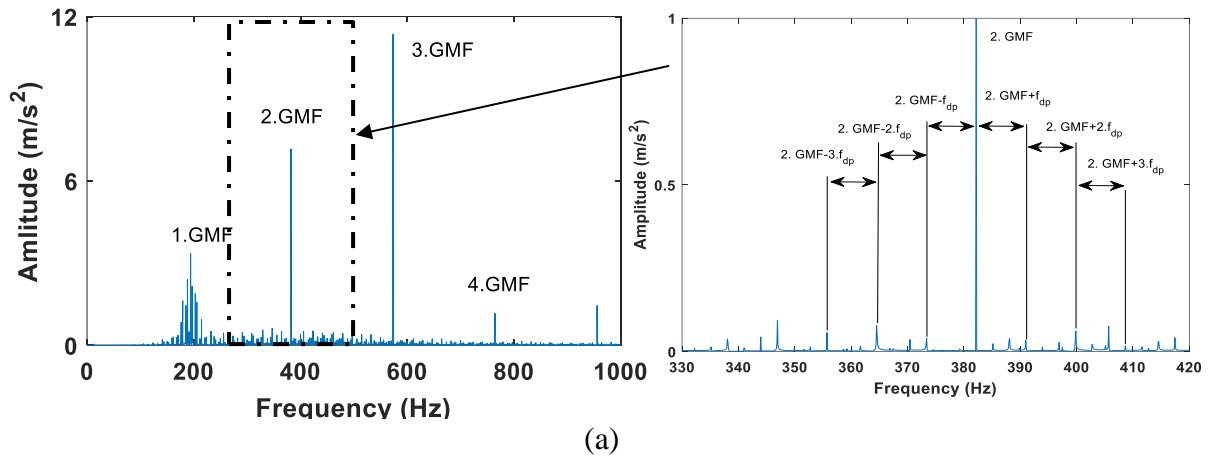


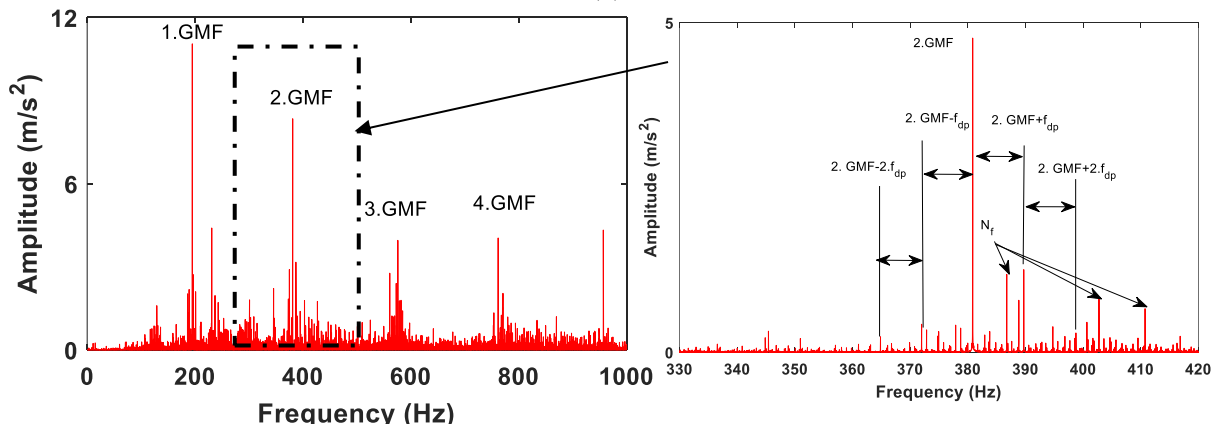
**Fig.10.** Time response (a) Simulated (b) Measured

We can assume that the time-domain analysis in this case is limited due to the complexity of the signal which make a difficulty to identify the defect period. For this reason, spectrum analysis is established (Fig. 11).

The signal associated with this kind of fault is modulated in amplitude due to the meshing, which leads to a complex spectrum characterized by the presence of lateral band spaced from  $f_{dp}$ .



(a)



(b)

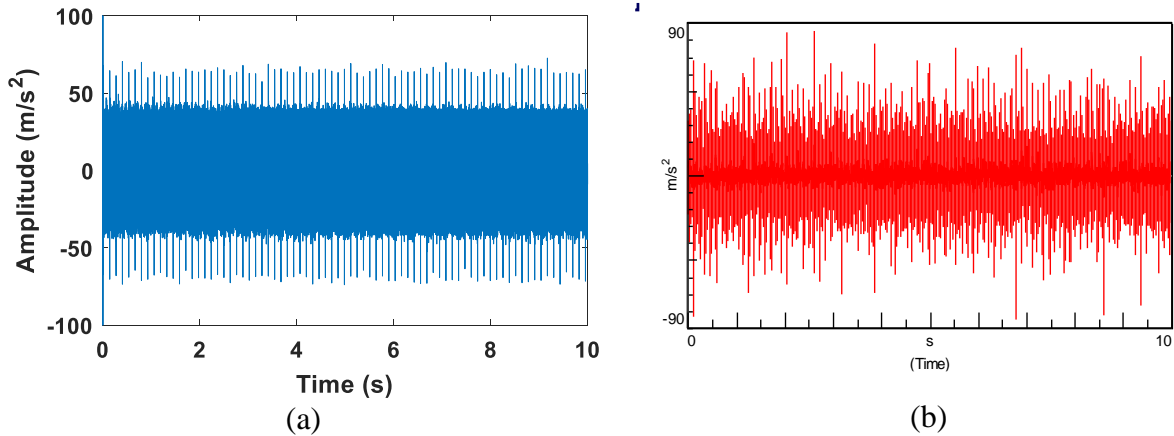
**Fig.11.** Spectrum (a) Simulated (b) Measured

It is noteworthy that the spectrum of the acceleration is dominated by the GMF and its harmonic. In fact, the GMF is modulated by the frequency of the defected planet and the frequency of the carrier multiplied by three (number of planets). Besides, the sidebands related to the defect are characterized by low amplitude due to the dimension of the defect. The frequency of the defected planet tooth is  $f_{dp}=1/T_{dp}$ , it is surrounded and equally spaced on GMF.

### c-Combined defect state: Crack & Spalling

The amplitude of vibration signal continue to increase as another kind of defects is added. The similar behaviour is shown for both simulation and experimental time signals. However, it is observable that Fig.12 (b) is much noisier than Fig.12 (a). This fact can be explained by the presence of an additional source of excitation and its effect on the components of the system. In the case of combined defect, the system is excited at least by three kind of excitation which are crack fault, spalling fault and the excitation of the motor. This fact can produce several phenomena and a variation on the behaviour of the system. Moreover, several coupled and critical modes could be excited. Additional functions could be also modified and amplified in this case such as the white noise function presented during experimental tests and neglected in the numerical model. In addition, the effect of the elastic coupling which is not considered in the developed model and the presence of assembly errors.

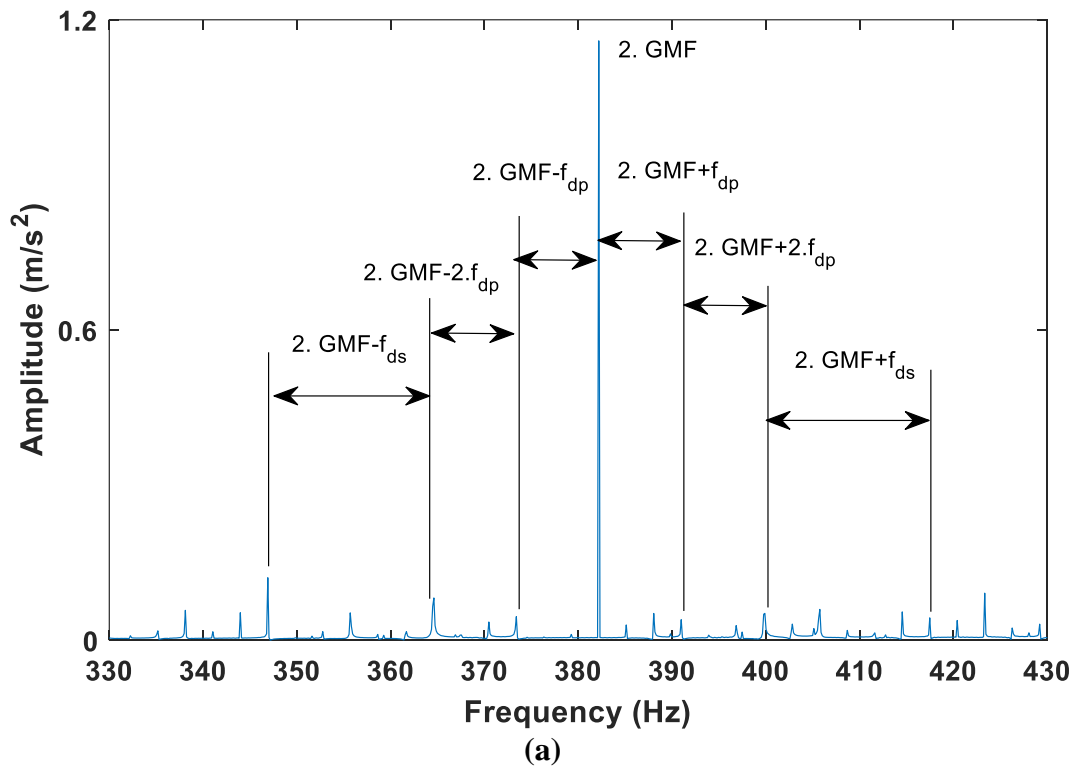
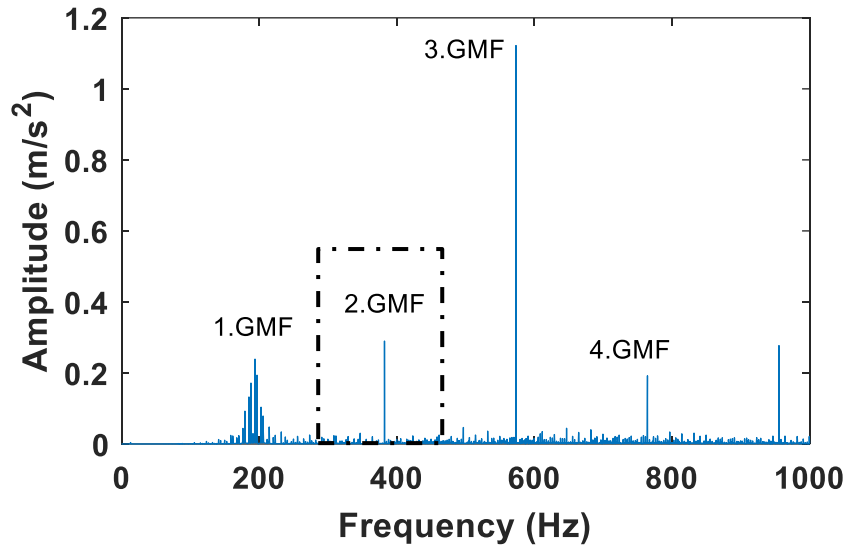
During each period of rotation of carrier, two categories of peaks are noticed in time responses: peaks related to the damaged sun and the others to the damaged planet.



**Fig.12.** Time response (a) Simulated (b) Experimental

The diagnosis-based times histories in the case of the combined defects is limited due to several parameters like the complexity of the structure where the majority of the components are in contact with each other's which can amplify vibration amplitude and cause more instability on the system. For this, the simulated and the measured quantities of accelerations were presented in the spectrum domain. The identification in this case is based on simple approach which is the kinematic configuration of the system as defined in the previous section. In this case where an additional cracked tooth added to the previous spalling defect, a new lateral band spaced by  $f_{ds}=1/T_{ds}$  could be identified in the spectrum of the acceleration and especially around the GMF and its harmonics.

Following the same approach, some frequencies characteristics of the planetary gear system like the frequency of the carrier could be identified on the spectrum and the GMF like in the case of single spalling defect condition. However, it is noticeable that the GMF is modulated at the same time by the frequency of the defected planet and the frequency of the carrier multiplied by three (number of planets). The amplitude of sidebands related to the defect is low due to the geometry of the defect.



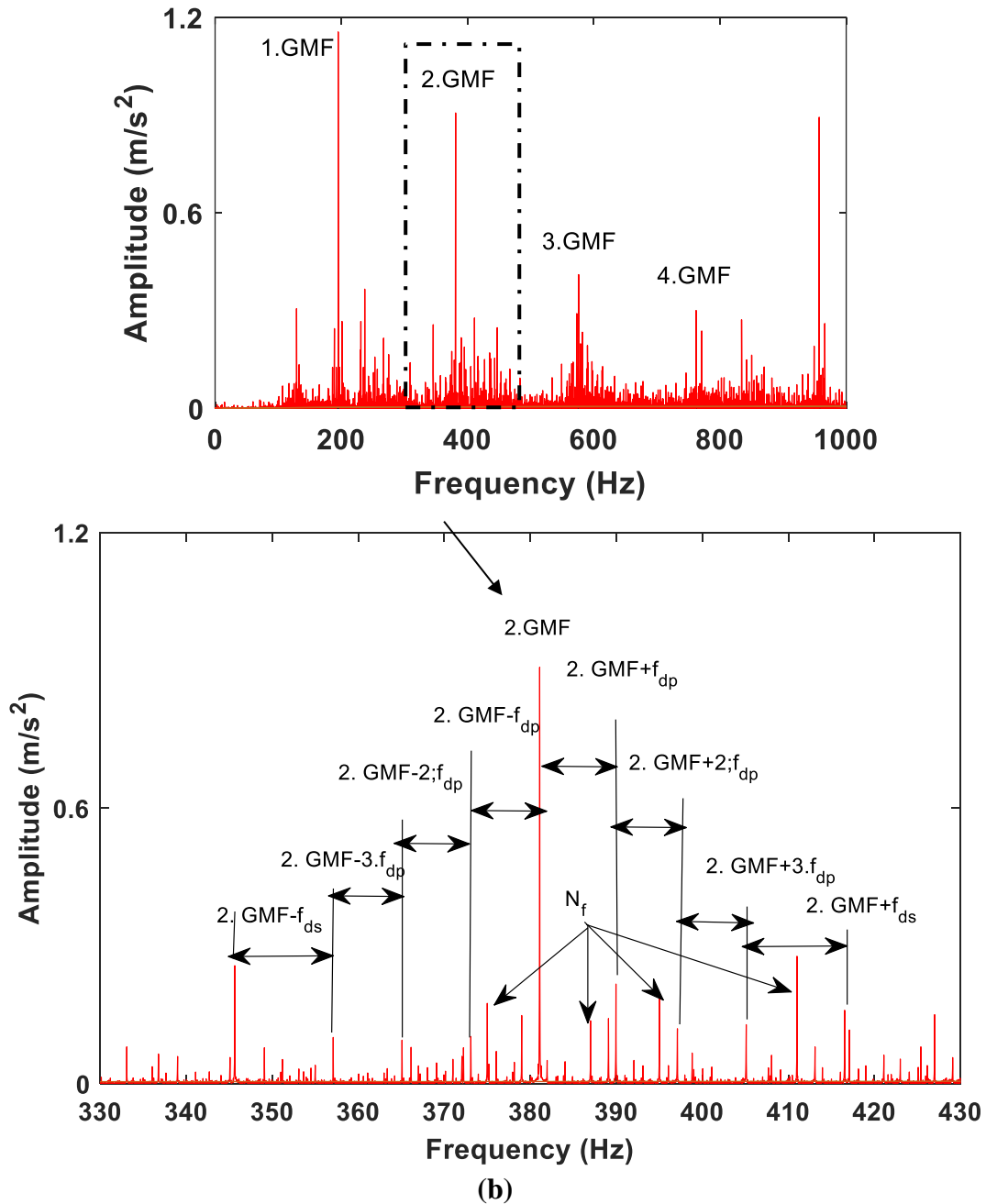


**Fig. 13.** Spectrum (a) Simulated (b) Measured

Fig. 13 indicates that the GMF is modulated by the frequency of the defected sun, the frequency of the defected planet defect and the frequency of the carrier multiplied by three (number of planets).

The apparition of two damage in a planetary gear system could be happen simultaneously and can cause a very bad scenario. It is also probably found more than two kind of defects. In this section, the impact of combined cracked and spalling tooth is discussed. The obtained results show that with the increasing of the number or the typos of defect, the dynamic behaviour of system change completely. This behaviour can also impact directly on several influencing functions such as damping and stiffness and can cause a degradation and a malfunction on the other mechanical components like shafts, rolling and coupling elements.

In fact, another category of sidebands is presented in the vibration spectrum which are explained by several influenced functions such as assembly errors and the phenomena of vibration transfer path, which was analysed by Hammami et al, [45].

### 5-2.2. Case of spalling planet during run up regime:

The impact of spalling defect is analysed in start-up regime, during this regime the bench is driven to 1000 rpm over 10 s and the response is measured on the test ring. The accelerations recorded experimentally and numerically show that the vibration level is directly proportional to the time as shown in Fig 14. Besides, a registered peak induced by the mesh of the damaged tooth. These pulses are presented during each meshing of the faulty tooth.

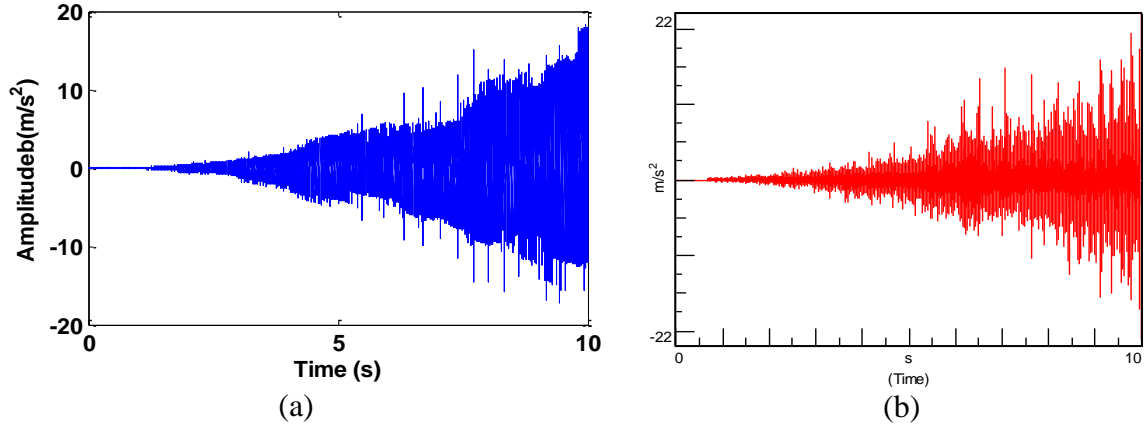


**Fig.14.** Time response (a) Simulated (b) Measured

As we know, the vibration feature frequencies will change along with rotation speed. To better observe the fault characteristics of vibration signal, it is reasonable and convenient to normalize all the frequencies by the carrier rotation frequency into order domain. After the normalized, the vibration feature frequencies will be associated with the structure parameters of planetary gear train and suppress the influence of nonstationary or time-varying rotation speed.

In fact, all the frequencies are normalized by carrier rotation frequency to obtain the corresponding feature orders.

After normalized to order domain, it can be obviously found that all frequencies become only connected with the physical parameters of planetary gear train as expressed in the following equation:

$$O_s = 1 + z_r / z_s \quad (10)$$

$$O_p = (z_p + z_r) / (z_s + z_r) \quad (11)$$

As mentioned before, the epicyclic gearbox is driven in start-up regime. Obviously, in this case, the period of defect is non-constant, so the frequency of the defect during this regime cannot be identified. For this, and in order to identify the orders associated to these faults, order maps are used.

The recorded signals give general information about the presence of the defect, but it did not indicate which component is faulty especially when the system runs under the non-stationary regime like the start up condition. For this reason, an angular method OTM is proposed to define the faulty component. This method resampled the raw signal with a uniform angle increment, which transforms the irregular signal in time-domain into regular periodic or quasi-periodic signal in the angle-domain as displayed in Fig.15.

The order speed presentation is dominated by the vibration components of the test ring gear which is the integer multiple orders (12.83, 25.66, ...) as listed in table 4.

**Table 4.** Orders characteristic of planetary gear components.

Type	Test		
Speed	0 – 1000 rpm		
Order of Natural frequency	5,11,27,34		
Components	P	C	S
Associated rotation order	2.4	1	5,06
Mesh order	12.8		

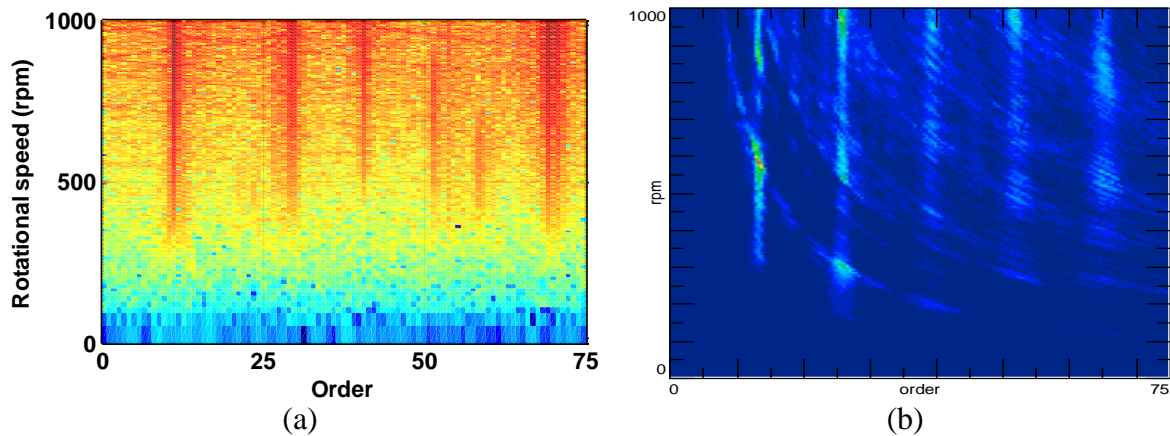


**Fig. 15.** Order map (a) Simulated (b) Measured

The vertical lines presented in Fig. 15 are related to the experimental and simulated meshing orders and they are harmonic.

To identify the order characteristic of the fault, a zoom around the first ten orders is achieved as illustrated in Fig. 16.

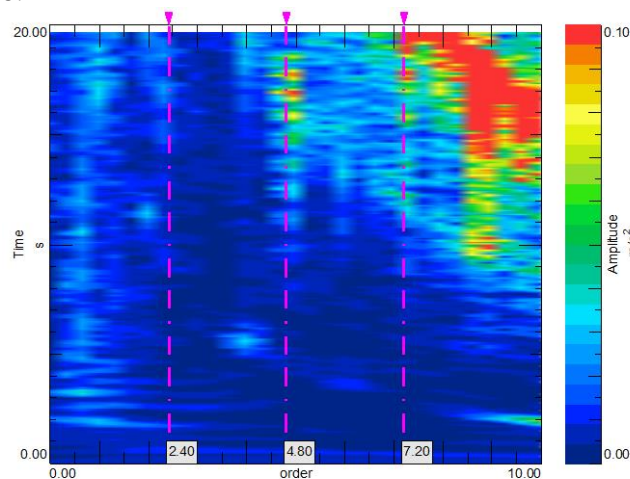


**Fig. 16.** Zoom around the first ten order of the acceleration

Fig.16 provides a significant result; it illustrates a harmonic order related to the damaged tooth of the planet components. The contact between the damaged tooth and the other teeth components lead an additional internal excitation function, this function is transferred to the sensor through a vibration path coming from the internal components and then matched on the external fixed components. The amplitude of this transfer function can be decreased in the transfer path due to several influenced factors like the tooth contact friction and the effects of the lubrication. Moreover, the low-intensity level is explained by the small geometry of the defect.

## 6- Discussions and conclusion

The investigation on the vibratory dynamic of the two planetary gears at damaged condition is analysed using measurement tests and simulations issued from the developed model. The frequency characterization of the system in stationary condition (fixed load and speed) has been featured. Two kinds of defect which are spalling, and crack defects are examined. The TVMS in presence of defects are modified by a progressive reduction of the TVMS which causes an amplitude modulation of the meshing frequency. The dynamic analysis-based vibration shows

efficiency for rotating machinery diagnosis and monitoring. The time vibration response in cases of stationary or non-stationary regimes demonstrates that the included system could defect under these conditions.

In steady state, the spectrum of acceleration defines properly the frequency of the defected teeth based on sidebands behaviour. Thus, the amplitude of those sidebands depends on the geometry of the defect.

In the case of a combined defect, two kinds of defect which are spalling, and crack defects are studied. The TVMS in presence of these defects are modified by a progressive reduction which causes an amplitude modulation of the GMF.

A dynamic analysis-based vibration is always a good option for rotating machinery diagnosis and monitoring. The time vibration response in cases of stationary regimes demonstrates that the system included defects.

The amplitude of the vibration response is sensitive to the number of the defects, the system vibration response amplitude increases in the case of the combined defects comparing to the healthy and the single defect condition.

The spectrum of acceleration during the stationary regimes define properly the frequency of the defected teeth based on sidebands appears around the mesh frequency. Thus, the amplitude of those sidebands depends on the geometry of the defect (sun or planet).

The impacts of defects are also analysed in the non-stationary condition during the run-up regime, by using OTM; the obtained results show that this method is very excellent to perform a good diagnosis in the cases of rotating machinery. The order associated with the spalled tooth is presented on the order map. The results developed numerically using the LPM and obtained experimentally are compared and correlated.

The dynamic behaviour of this system and in presence of defect still needs to be deeply studied using not only various speeds but also variable speed and variable loading condition.

### **Acknowledgements**

“The authors would like to acknowledge Project DPI2017-85390-P funded by the Spanish Ministry of Economy, Industry, and Competitiveness for supporting this research.”

Acknowledgment to the University of Cantabria cooperation project for doctoral training of University of Sfax's students.

### **References**

- [1] Zhang, M., Wang, K., Wei, D. and Zuo, M.J., 2018. Amplitudes of characteristic frequencies for fault diagnosis of planetary gearbox. *Journal of Sound and Vibration*, 432, pp.119-132.
- [2] Gelman, L., Zimroz, R., Birkel, J., Leigh-Firbank, H., Simms, D.M., Waterland, B. and Whitehurst, G., 2005. Adaptive vibration condition monitoring technology for local tooth damage in gearboxes.
- [3] H. Ma, J. Zeng, R. Feng, X. Pang, Q. Wang, B. Wen, Review on dynamics of cracked gear systems, *Eng. Fail. Anal.* 55 (2015) 224–245.
- [4] L. Fan, S. Wang, X. Wang, F. Han, H. Lyu, Nonlinear dynamic modeling of a helicopter planetary gear train for carrier plate crack fault diagnosis, *Chin. J.Aeronaut.* 29 (2016) 675–687.
- [5] Chaari, F., Fakhfakh, T., & Haddar, M. (2009). Analytical modelling of spur gear tooth crack and influence on gearmesh stiffness. *European Journal of Mechanics-A/Solids*, 28(3), 461-468.
- [6] Liang, X., Zhang, H., Liu, L., & Zuo, M. J. (2016). The influence of tooth pitting on the mesh stiffness of a pair of external spur gears. *Mechanism and Machine Theory*, 106, 1-15.
- [7] H. Ma, Z. Li, M. Feng, R. Feng, B. Wen, Time-varying mesh stiffness calculation of spur gears with spalling defect, *Eng. Fail. Anal.* 66 (2016) 166–176.

- [8] A. Saxena, A. Parey, M. Chouksey, Time varying mesh stiffness calculation of spur gear pair considering sliding friction and spalling defects, *Eng. Fail. Anal.* 70 (2016) 200–211.
- [9] Lewicki, D. G. (2002). Gear Crack Propagation Path Studies-Guidelines for Ultra-Safe Design. *Journal of the American Helicopter Society*, 47(1), 64-72.
- [10] Chaari, F., Fakhfakh, T., & Haddar, M. (2006). Dynamic analysis of a planetary gear failure caused by tooth pitting and cracking. *Journal of Failure Analysis and Prevention*, 6(2), 73-78.
- [11] Liu, J., Wang, L., Ma, J., Yu, W., & Shao, Y. (2019). A multi-body dynamic study of vibration of a planetary gear train with the planetary bearing fault. *Proceedings of the Institution of Mechanical Engineers, Part K: Journal of Multi-body Dynamics*, 233(3), 677-695.
- [12] R. Ma, Y. Chen, Research on the dynamic mechanism of the gear system with local crack and spalling failure, *Eng. Fail. Anal.* 26 (2012) 12–20.
- [13] Z. Cheng, N. Hu, X. Zhang, Crack level estimation approach for planetary gearbox based on simulation signal and GRA, *J. Sound Vib.* 331 (2012) 5853–5863.
- [14] Z. Tian, M.J. Zuo, S. Wu, Crack propagation assessment for spur gears using model-based analysis and simulation, *J. Intell. Manuf.* 23 (2012) 239–253.
- [15] X. Liang, M.J. Zuo, Investigating vibration properties of a planetary gear set with a cracked tooth in a planet gear, in: Fort Worth, Texas, 2014, pp. 568–575.
- [16] G. Li, F. Li, Y. Wang, D. Dong, Fault diagnosis for a multistage planetary gear set using model-based simulation and experimental investigation, *ShockVib.* 2016 (2016) 1–19.
- [17] Ryali, L., & Talbot, D. (2021). Dynamic load distribution of planetary gear sets subject to both internal and external excitations. *Forschung im Ingenieurwesen*, 1-12.
- [18] Chen ZG, Shao YM. Dynamic simulation of spur gear with tooth root crack propagating along tooth width and crack depth. *Eng Fail Anal* 2011;18:2149–64.
- [19] Mohammed OD, Rantatalo M, Aidanpaa J, et al. Vibration signal analysis for gear fault diagnosis with various crack progression scenarios. *Mech Syst Signal Process* 2013;41:17695.
- [20] Wu SY, Zuo MJ, Parey A. Simulation of spur gear dynamics and estimation of fault growth. *J Sound Vib* 2008;317:608–24.
- [21] Mohammed OD, Rantatalo M, Aidanpaa JO. Dynamic modeling of a one-stage spur gear system and vibration-based tooth crack detection analysis. *Mech Syst Signal Process* 2015;54–55:293–305.
- [22] Zhou XJ, Shao YM, Lei YG, et al. Time-varying meshing stiffness calculation and vibration analysis for a 16DOF dynamic model with linear crack growth in a pinion. *J Vib Acoust* 2012;134:011011.1–011011.11.
- [23] Howard I, Jia SX, Wang JD. The dynamic modeling of a spur gear in mesh including friction and a crack. *Mech Syst Signal Process* 2001;15:831–53.
- [24] J. Zhang, J. S. Dhupia, C. J. Gajanayake, Stator Current Analysis From Electrical Machines Using Resonance Residual Technique to Detect Faults in Planetary Gearboxes, *IEEE Transactions on Industrial Electronics* 62 (9) (2015) 5709{5721. doi:10.1109/TIE.2015.2410254.
- [25] S. H. Kia, H. Henao, G. A. Capolino, Fault Index Statistical Study for Gear Fault Detection Using Stator Current Space Vector Analysis, *IEEE Transactions on Industry Applications* 52 (6) (2016) 4781{4788. doi:10.1109/TIA.2016.2600596.
- [26] Leaman, F., Baltes, R., & Clausen, E. (2021). Comparative case studies on ring gear fault diagnosis of planetary gearboxes using vibrations and acoustic emissions. *Forschung im Ingenieurwesen*, 85(2), 619-628.
- [27] A. Glowacz, W. Glowacz, Vibration-based fault diagnosis of commutator motor, *Shock and Vibration* 2018 (2018) 1{10.
- [28] L. S. Dhamande, M. B. Chaudhari, Compound gear-bearing fault feature extraction using statistical features based on time-frequency method, *Measurement* 125 (2018) 63{77.

- [29] C. Wang, M. Gan, C. Zhu, A supervised sparsity-based wavelet feature for bearing fault diagnosis, *Journal of Intelligent Manufacturing* (2016) 1{11.
- [30] C. Wang, M. Gan, C. Zhu, Fault feature extraction of rolling element bearings based on wavelet packet transform and sparse representation theory, *Journal of Intelligent Manufacturing* 29 (4) (2018) 937{951.
- [31] C. Wu, T. Chen, R. Jiang, L. Ning, Z. Jiang, A novel approach to wavelet selection and tree kernel construction for diagnosis of rolling element bearing fault, *Journal of Intelligent Manufacturing* 28 (8) (2017)1847{1858.
- [32] V. C. M. N. Leite, J. G. B. d. Silva, G. F. C. Veloso, L. E.B. d. Silva, G. Lambert-Torres, E. L. Bonaldi, L. E. d. L. d. Oliveira, Detection of Localized Bearing Faults in Induction Machines by Spectral Kurtosis and Envelope Analysis of Stator Current, *IEEE Transactions on Industrial Electronics* 62 (3) (2015) 1855{1865. doi:10.1109/TIE.2014.2345330.
- [33] S. Singh, N. Kumar, Detection of Bearing Faults in Mechanical Systems Using Stator Current Monitoring, *IEEE Transactions on Industrial Informatics* 13 (3) (2017) 1341{1349. doi:10.1109/TII.2016.2641470.
- [34] L. Hong, J. S. Dhupia, A time domain approach to diagnose gearbox fault based on measured vibration signals, *Journal of Sound and Vibration* 333 (7) (2014) 2164{2180. doi:10.1016/j.jsv.2013.11.033.
- [35] S. Fedala, D. Remond, R. Zegadi, A. Felkaoui, Contribution of angular measurements to intelligent gear faults diagnosis, *Journal of Intelligent Manufacturing* 29 (5) (2018) 1115{1131.
- [36] Park, J., Ha, J. M., Youn, B. D., Leem, S. H., Choi, J. H., & Kim, N. H. (2014). Model-based fault diagnosis of a planetary gear using transmission error. In *Annual Conference of the PHM Society* (Vol. 6, No. 1).
- [37] Li, G., Li, F., Wang, Y., & Dong, D. (2016). Fault diagnosis for a multistage planetary gear set using model-based simulation and experimental investigation. *Shock and Vibration*, 2016.
- [38] Li, G., Liang, X., & Li, F. (2018). Model-based analysis and fault diagnosis of a compound planetary gear set with damaged sun gear. *Journal of Mechanical Science and Technology*, 32(7), 3081-3096.
- [39] Sang, M., Huang, K., Xiong, Y., Han, G., & Cheng, Z. (2021). Dynamic modeling and vibration analysis of a cracked 3K-II planetary gear set for fault detection. *Mechanical Sciences*, 12(2), 847-861.
- [40] Mbarek, A., Hammami, A., Del Rincon, A. F., Chaari, F., Rueda, F. V., & Haddar, M. (2017). Effect of load and meshing stiffness variation on modal properties of planetary gear. *Applied Acoustics*.
- [41] Mbarek, A., Del Rincon, A. F., Hammami, A., Iglesias, M., Chaari, F., Viadero, F., & Haddar, M. (2018). Comparison of experimental and operational modal analysis on a back to back planetary gear. *Mechanism and Machine Theory*, 124, 226-247.
- [42] Mbarek, A., Hammami, A., Del Rincon, A. F., Chaari, F., Rueda, F. V., & Haddar, M. (2017, March). Effect of Gravity of Carrier on the Dynamic Behavior of Planetary Gears. In *International Conference Design and Modelling of Mechanical Systems* (pp. 975-983). Springer, Cham.
- [43] Dhatt, G., Touzot, G. and Lefrançois, E. (2005) Méthode des Éléments Finis – Une Présentation, Hermès Science Publications, Paris, France.
- [44] Hammami A, Del Rincon AF, Chaari F, Santamaria MI, Rueda FV, Haddar M (2016) Effects of variable loading conditions on the dynamic behaviour of planetary gear with power recirculation. *Measurement* 94:306–315
- [45] Hammami, A., del Rincon, A. F., Chaari, F., Rueda, F. V., & Haddar, M. (2017, April). Transfer Path Analysis of Planetary Gear with Mechanical Power Recirculation. In *Signal*

Processing Applied to Rotating Machinery Diagnostics,(SIGPROMD'2017) (pp. 104-115).  
Springer, Cham.